Improved Heart Rate Tracking Using Multiple Wrist-type Photoplethysmography during Physical Activities

Lianning Zhu, Dongping Du, *Member, IEEE*

***Abstract*—Photoplethysmography (PPG) signals collected from wearable sensing devices during physical exercise are easily corrupted by motion artifact (MA), which poses greatly challenge on heart rate (HR) estimation. This paper proposes a new framework to accurately estimate HR using two leads of PPG signals in combination with accelerometer (ACC) data in the present of MA. A moving time window is first used to segment PPG signals and ACC signals. Then, MA are attenuated by joint sparse spectrum reconstruction in each time window, where maximum spectrum frequencies of ACC are subtracted from the spectrum frequency of PPG signals. Further, HR for each cleansed PPG is estimated from the frequency with maximum amplitude in the sparse spectrum. The actual HR is determined using spectral band powers calculated from each reconstructed PPG signals. The proposed method was validated using the 2015 IEEE Signal Processing Cup dataset. The average absolute error is 1.15 beats per minutes (BPM) (standard deviation: 2.00 BPM), and the average absolute error percentage is 0.95% (standard deviation: 1.86%). The proposed method outperforms the previously reported work in terms of accuracy.**

I. Introduction

Physical exercise can greatly benefit cardiac patients for effective post-operative management of heart health and improving patients' quality of life (QoL). However, it is important to closely monitor patients' condition during the exercise to ensure safety and prevent life threatening events. Electrocardiogram (ECG) is a traditional measurement of cardiac activity, where multiple sensors are attached to chest and arms to record the electrical activity of the heart. However, wearing the electrodes is not comfortable, and the procedure is hard to operate by patients themselves at home. Wearable monitors such as wristband become a promising alternative for physical exercise monitoring of cardiac patients in home environment because they are small, convenient, and at low cost. The monitors can provide multiple leads of Photoplethysmography (PPG) signals, which are obtained using a pulse oximeter that illuminates the skin and measures changes in light absorption [1]. The PPG signals can be effective parameters for estimating HR. However, PPG recordings are often contaminated by different factors, e.g., environmental artifacts, experimental error, and physiological artifacts [2]. Environmental artifacts can be easily eliminated using filters, but experimental errors and physiological artifacts are caused by subjects' motion, which are hard to separate.

Many techniques have been developed to remove motion artifact (MA). Given the fact that there are frequency overlaps between the clean PPG signals and MA, studies have been done to eliminate MA while minimizing the data lose. Common techniques include adaptive filtering [2, 3], empirical mode decomposition [2], Kalman filtering [4], and spectrum subtraction [5, 6]. Noted that most of these techniques only apply to signals with weak MA. To address the limitation, Zhang [7] proposed a new MA removal method based on Joint Sparse Spectrum reconstruction (JOSS), which assumes that the spectra of PPG signals and simultaneous ACC signals have the same structure. Multiple measurement vector (MMV) model was used to estimate sparse spectra of the combination of each PPG signal and ACC signals. This helps to recover unique solution and identify spectral peaks with smaller error comparing to the single measurement vector model. In this paper, we adopted JOSS technique to remove MA. However, to improve the HR estimation, we propose to use two lead PPG signals to jointly track HR.

Although JOSS is efficient in removing MA, there are still residual MA in the PPG signals, which still challenges HR monitoring. Therefore, efficient HR monitoring techniques are demanded. Various HR estimation algorithms have been developed in the literature, which include zero-crossing count [8], dominant frequency detection [8], and adaptive frequency tracking [3], spectral peak detection based on sparse signal reconstruction [6] and Bayesian decision theory [5]. Zero-crossing count and dominant frequency detection are not robust when MA interfere is strong. Adaptive frequency tracking can track instantaneous frequency, but the results depend greatly on filter parameters and initial conditions. Spectral peak detection based on Bayesian decision theory [5] overcomes some drawbacks of traditional power spectrum estimation. However, it relies too much on previous estimated HR. In addition, [7] has the same limitations and involves too many arbitrarily defined constraints.

In our study, we propose a new framework for efficient HR monitoring with less arbitrarily defined constraints. Reconstructed PPG signals were obtained after MA removal using JOSS. HRs of two leads PPG signals in a sliding time window were estimated by finding the frequency with maximum amplitude in sparse spectra of each reconstructed PPG signal in the same time window. Then spectral band power is calculated to determine final HR in the same time window. To prevent biased HR detection, moving average filter [5] and a smoother algorithm [10] were used for post-processing. The flow chart of the proposed method is shown in Figure 1.

This paper is organized as follows. Section II introduces the research method. Experimental results are shown in section III, where the efficiency and robustness of proposed method will be discussed. Conclusions are drawn in section IV.

*Research supported by National Science Foundation (CMMI-1646664, and CMMI-1728338).

L. Zhu, D. Du. are with the Department of Industrial, Manufacturing, & Systems Engineering, Texas Tech University, Lubbock, TX 43061 USA. Phone: 806-834-7388. (e-mail: dongping.du@ttu.edu).

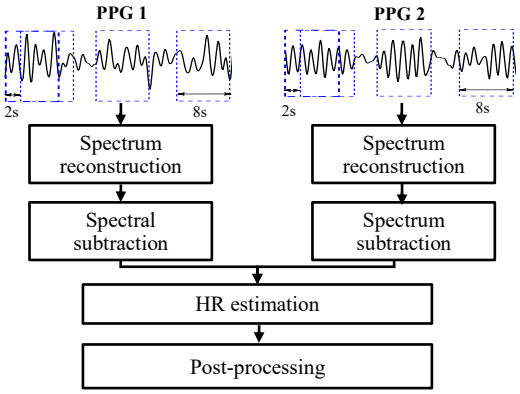

Figure 1. Flow chart of proposed framework

II. METHODS

A. Data

The method proposed in this work is developed and validated using the 2015 IEEE Signal Processing Cup data [6]. This data are composed of 12 training recordings from 12 subjects. The subjects are at the ages of 18-35 year old. Recording for each subject includes one-channel ECG signals, two-channel PPG signals, and three-axis ACC signals. All signals are sampled at 125Hz. For the 12 training dataset, the subjects were required to run at different speeds. Please see [6] for detailed speed protocols.

Before MA removal and HR estimation, all signals were first filtered with a band-pass filter at 0.5 and 5 Hz, then down-sampled to 25 Hz in order to smooth signals and reduce computing time. Further, a sliding time window is applied to truncate all signals into segments. The length of time window is 8 seconds and the moving step is 2 seconds. MA removal and HR estimation were performed in each time window. All segments were normalized to same variance to ensure consistent energy.

B. Joint Sparse Reconstruction (JOSS) Using the Multiple Measurement Vector (MMV) model

The sparse spectra of the PPG and the ACC signals were estimated using multiple measurement vector (MMV) model [7], which is described as follows:

$$\boldsymbol{Y} = \boldsymbol{\Phi X} + \boldsymbol{V} \tag{1}$$

where $\boldsymbol{Y} \in \mathbb{R}^{M\times L}$ is the matrix consisting of L measurement vectors, $\boldsymbol{\Phi} \in \mathbb{C}^{M\times N}$ is the redundant discrete Fourier transform (DFT) basis, $\boldsymbol{X} \in \mathbb{C}^{N\times L}$ is the desired solution matrix, and $\boldsymbol{V} \in \mathbb{R}^{M\times L}$ is noise matrix. The redundant DFT basis is chosen as:

$$\Phi_{m,n} = e^{j\frac{2\pi}{N}mn}, m = 0, \dots, M-1; n = 0, \dots, N-1 \tag{2}$$

where $\Phi_{m,n}$ denotes the element in m^{th} row and n^{th} column of $\boldsymbol{\Phi}$. It is assumed that the solution matrix $\boldsymbol{X}$ is row-wise sparse, i.e., most rows in $\boldsymbol{X}$ are zero.

In this paper, we combined segments of each PPG signal and the corresponding ACC signals to form the measurement matrix $\boldsymbol{Y}$. Each column of $\boldsymbol{X}$, i.e., $\boldsymbol{x}_i$, i=1…4, is Fourier transform of corresponding signal $\boldsymbol{y}_i$, i=1…4, in $\boldsymbol{Y}$. M is the length of segments and N is set to be 1024. Regularized M-FOCUSS algorithm [9] was used to obtain the sparse matrix $\boldsymbol{X}$. We chose M-FOCUSS as it is computationally efficient and could provide reliable solution when $\boldsymbol{\Phi}$ is highly coherent.

C. Spectral Subtraction for Motion Artifact Removal

Sparse spectra of raw PPG signal and ACC signals were obtained using MMV model. MA was removed following the steps presented blew.

1. For each frequency bin, maximum spectral coefficient in ACC spectra was chosen as spectral coefficient of MA.
2. For the same frequency bin, spectral coefficient in PPG spectrum was subtracted by spectral coefficient of MA.
3. Negative spectral coefficients in PPG spectrum were set to 0 to obtain cleansed PPG spectrum.

D. Heart Rate Estimation

There are two steps to estimate HR in each time window. First, HR was estimated from each cleansed PPG spectrum. Second, spectral band power was calculated to determine global HR. Details of each step are given as follows.

First Step. Following the steps discussed in Section B and C, a cleansed PPG spectrum was obtained for each PPC signal in a sliding window. The frequency with maximum amplitude, i.e., $f_{i,max}$, i=1, 2, was chosen to be the HR frequency of each PPG signal. HR was calculated by multiplying HR frequency with 60s. There were two channels of PPG signals. Correspondingly, two HRs in the same time window were identified in this step. The true heart rate will be determined based on the two candidate HRs, which will be introduced in the second step.

Second Step. As above mentioned, in each time window, two candidate HRs were used to determine the true HR, written as HR_t. Let define the two candidate HRs as HR_i, i= 1, 2, which was derived from the i^{th} PPG signal. In addition, a new set of PPG signals was reconstructed from the cleansed PPG spectrum obtained in Section C, which was further used for HR estimation (See Fig. 2).

For each reconstructed PPG signal in a sliding time window, a parameter ω_i, i = 1, 2, was used to indicate the quality of the candidate HR estimation from i^{th} PPG signal. The parameter ω_i, was determined by band powers. Two frequency bands were defined using the frequency, $f_{i,max}$, from first step, and a bandwidth of 0.32Hz is applied. As seen in Figure 2, the first band covers the frequency range of [$f_{1,max}$-0.16, $f_{1,max}$+0.16], and the second band covers the frequency range of [$f_{2,max}$-0.16, $f_{2,max}$+0.16]. Further, for i^{th} reconstructed PPG signal, the jth band power b_{ij}, i=1, 2, j=1, 2, was calculated. If the estimated candidate HR value is in good quality, ω_i is set to be 1, otherwise, ω_i is set to be ε, $\varepsilon \to 0$. As shown in Figure 2, ω_1 equals to 1 when b_{11}>b_{12}, otherwise, ω_1= ε. Similarly, ω_2 equals to 1 when b_{22}>b_{21}, otherwise, ω_2= ε. The rationale is that the estimated candidate HR value with higher band power is likely to be true. Using ω_i, the true estimated HR value can be determined as

$$HR_t = \frac{\omega_1}{\omega_1+\omega_2} HR_1 + \frac{\omega_2}{\omega_1+\omega_2} HR_2.$$

This procedure was used for the signals in the first six sliding time windows to obtain reliable estimation of the HR. To reduce the computational time, for the signal in the remaining time windows, we assumed that at least one of two

candidate HRs was close to true HR, and HR should not change dramatically in short time. Therefore, the true HR is determined by referencing to the average heart rate, denoted as $\overline{HR}$, of six previous successive time windows. The true HR index k was found as:

$$k = \min_{i=1,2}(abs(HR_i - \overline{HR}))$$

where the HR that is closer to the average heart rate $\overline{HR}$ is chosen. If the difference between chosen HR and $\overline{HR}$ is larger than 30 BPM, $\overline{HR}$ is chosen as true estimated HR.

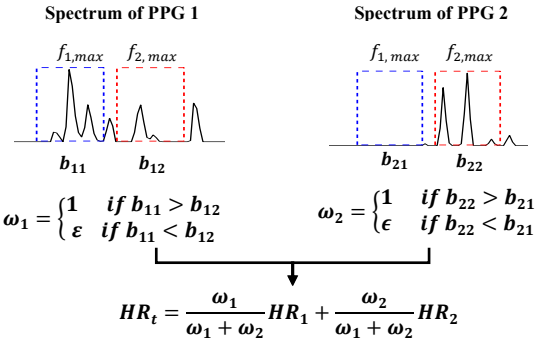

Figure 2. Flow chart of HR estimation

E. Post-processing

After HR estimation, post-processing was performed to correct wrong HR estimation because recorded PPG signals may not provide accurate information due to MA and HR should not change dramatically in short time for healthy subjects. Moving average filter [5] and a smoother algorithm [10] were used for this purpose.

Moving average filter For ith estimated HR, the average heart rate $\overline{hr_i}$ and standard deviation σ_i are given by:

$$\overline{hr_i} = \frac{1}{10}\sum_{j=i-5}^{i+4} hr_i$$

$$\sigma_i = \sqrt{\frac{1}{10}\sum_{j=i-5}^{i+4}(hr_i - \overline{hr_i})}.$$

When difference between $\overline{hr_i}$ and hr_i is greater than σ_i, hr_i is discarded and replaced by $\overline{hr_i}$. The first five and last four estimated true HR values were not checked by moving average filter. Therefore, a smoother algorithm was used for these HR values, which is described as follows.

Smoother algorithm For ith estimated HR_i, the smoother algorithm was performed on HR_i and the subsequent nine HR values if HR_i is from the first five estimated true HR values. Otherwise, this algorithm was performed on HR_i and previous nine HR values. If the relative error between HR_i and corresponding smoothed HR_i was larger than 10%, HR_i was replaced by the corresponding smoothed HR_i.

III. Results

A. Algorithm Validation

To evaluate the performance of the proposed algorithm, two parameters were measured, i.e., average absolute error, and average absolute. The average absolute error (in BPM (beats per minutes)), is given by:

$$Error1 = \frac{1}{L}\sum_{i=1}^{L} |BPM_{est}(i) - BPM_{true}(i)|$$

, and the average absolute error percentage is given by:

$$Error2 = \frac{1}{L}\sum_{i=1}^{L} \frac{|BPM_{est}(i) - BPM_{true}(i)|}{BPM_{true}(i)}$$

where $BPM_{est}(i)$ was the HR estimated from the proposed algorithm, and $BPM_{true}(i)$ was the true HR estimated from subjects' ECG recordings for validation purpose, L was the number of HR estimates.

B. Experimental Results

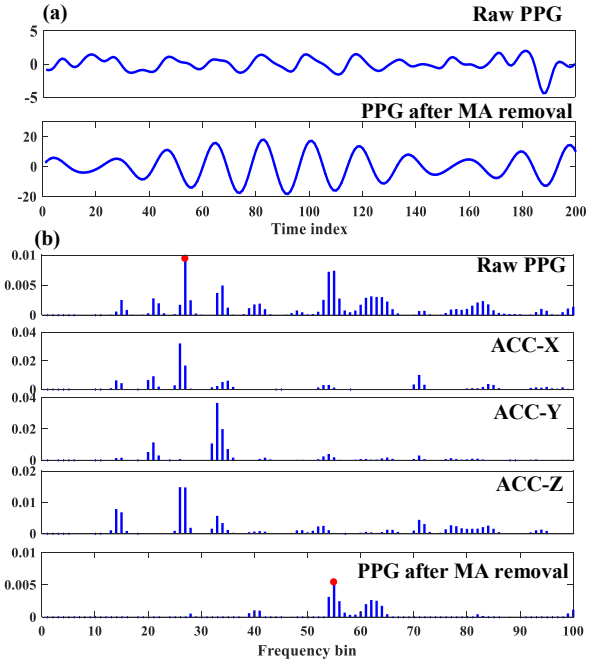

Figure 3. Effect of MA removal on data segment. (a) Raw PPG signal and PPG signal after MA removal; (b) Sparse spectrum of raw PPG, ACC signals and PPG signal after MA removal.

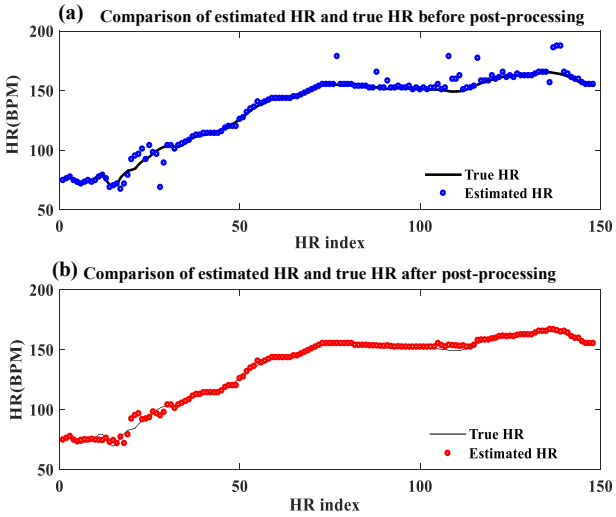

Figure 4. Comparison of estiamted HR values before and after post-processing with true HR values

To show the performance of the MA removal algorithm, comparisons of raw PPG and PPG signal after MA removal in both time domain and frequency domain were shown in Figure 3. The red dots represented frequencies with maximum

amplitude. ACC signals in frequency domain were also provided to show the relationship of PPG and ACC signals. From Figure 3, we can see that frequencies of were identified and removed from the raw PPG signals. The frequency that is not correlated with ACC signals were retained, which provide a clear rhythm of PPG signal.

To display performance of HR estimation, the estimated HRs for an entire PPG signal before and after post-processing were provided for comparison. As shown in Figure 4 (a), the black solid line shows the true HR, and the blue circles show the HR estimated using the proposed algorithm. In Figure 4 (b), we presented the post-processed HRs (i.e., red dots) and the true HR (i.e., black solid line). As seen in the Figure, our estimations match well with the true HR, which validates the effectiveness of the proposed framework.

TABLE I. ERROR 1 AND ERROR 2 RESULTS

Record	ERROR 1 (BPM)			ERROR 2 (%)		
	JOSS [7]	*[3]*	*OUR WORK*	*JOSS [7]*	*[3]*	*OUR WORK*
1	1.33	1.75	1.38	1.19	1.59	1.25
2	1.75	1.94	1.41	1.66	1.99	1.38
3	1.47	1.17	1.37	1.27	1.02	1.22
4	1.48	1.67	1.20	1.41	1.51	1.08
5	0.69	0.95	0.97	0.51	0.75	0.77
6	1.32	1.22	1.18	1.09	1.05	0.94
7	0.71	0.91	0.80	0.54	0.72	0.60
8	0.56	1.17	0.93	0.47	1.04	0.84
9	0.49	0.87	0.84	0.41	0.76	0.74
10	3.81	2.95	1.59	2.43	1.93	1.03
11	0.78	1.15	1.22	0.51	0.79	0.84
12	1.04	1.00	0.95	0.81	0.79	0.71
Average	1.28	1.40	1.15	1.01	1.16	0.95
Total	2.61		2.00	2.29		1.86

To evaluate proposed method, the average absolute error (Error 1) and average absolute error percentage (Error 2) on training dataset were compared with Error 1 and Error 2 in [7] and [3], which were shown in Table I. SD is standard deviation of estimated HR values over all datasets, and average shows mean error of the 12 records. As see in Table I, our algorithm provides lower errors as compared to JOSS in [7] and adaptive filter with frequency tracking in [3]. The absolute estimation error (Error 1) of our work was 1.15±2.00 BPM (mean ± standard deviation) and error percentage (Error 2) was 0.95%±1.86%. In contrast, Error 1 and Error 2 of JOSS [7] was 1.28±2.61 BPM and 1.01%±2.29%. Error 1 and Error 2 in [3] was 1.40 BPM and 1.16%. The SD was not provided in [3].

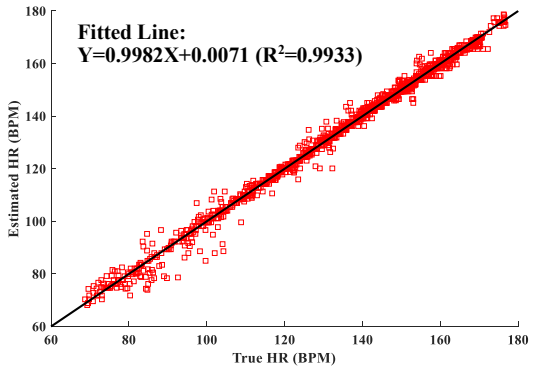

Figure 5. Scatter plot between true HR values and estimated HR values with fitted line.

To further demonstrate the effectiveness of our method, the scatter plot of true HR and estimated HR over all datasets was shown in Figure 5. A straight line, i.e., $Y = 0.9982X + 0.0071$ was fitted to the scatter points, where X was true HR and Y was estimated HR. R square was measured as 0.9933 in our work, which is slightly better as compared to the R square of 0.993 in [7]. The closer the coefficient of X is to one, the better the estimated HR values are. Note that the coefficient of X in [7] were 0.991, which is smaller than our coefficients of 0.9982. This further demonstrated the superior performance of the proposed method.

IV. CONCLUSION

In this study, a new HR estimation algorithm using wrist-type PPG during physical exercise was presented. First, joint sparse spectrum reconstruction was used to remove MA. Second, HR was estimated based on multiple reconstructed PPG signals. Third, post-processing procedure is applied to correct wrong estimations. The proposed algorithm was compared with a recent study, which showed superior performance. There are only a few arbitrary defined constraints in our method. It focused more on information from recorded signals themselves and could reduce arbitrary error and improve reliability of results. In addition, the data was down-sampled and HR estimation process was computationally efficient. Therefore, it has the potential for online monitoring. In other words, this method reduces signal processing time and could be applied to wearable devices. One limitation of the proposed method is that average heart rate of previous consecutive windows was used as reference for current estimation. Therefore, the HR tracking accuracy could be affected by previous estimations.

REFERENCES

[1] Allen, J., Photoplethysmography and its application in clinical physiological measurement. Physiological measurement, 2007. 28(3): p. R1.

[2] Sweeney, K.T., T.E. Ward, and S.F. McLoone, Artifact removal in physiological signals—Practices and possibilities. IEEE transactions on information technology in biomedicine, 2012. 16(3): p. 488-500.

[3] Fallet, S. and J.-M. Vesin, Robust heart rate estimation using wrist-type photoplethysmographic signals during physical exercise: an approach based on adaptive filtering. Physiological measurement, 2017. 38(2): p. 155.

[4] Seyedtabaii, S. and L. Seyedtabaii, Kalman filter based adaptive reduction of motion artifact from photoplethysmographic signal. World Acad. Sci. Eng. Technol, 2008. 37: p. 173-176.

[5] Sun, B. and Z. Zhang, Photoplethysmography-based heart rate monitoring using asymmetric least squares spectrum subtraction and bayesian decision theory. IEEE Sensors Journal, 2015. 15(12): p. 7161-7168.

[6] Zhang, Z., Z. Pi, and B. Liu, TROIKA: A general framework for heart rate monitoring using wrist-type photoplethysmographic signals during intensive physical exercise. IEEE Transactions on Biomedical Engineering, 2015. 62(2): p. 522-531.

[7] Zhang, Z., Photoplethysmography-based heart rate monitoring in physical activities via joint sparse spectrum reconstruction. IEEE transactions on biomedical engineering, 2015. 62(8): p. 1902-1910.

[8] Vogel, S., et al. In-ear heart rate monitoring using a micro-optic reflective sensor. in Engineering in Medicine and Biology Society, 2007. EMBS 2007. 29th Annual International Conference of the IEEE. 2007. IEEE.

[9] Cotter, S.F., et al., Sparse solutions to linear inverse problems with multiple measurement vectors. IEEE Transactions on Signal Processing, 2005. 53(7): p. 2477-2488.

[10] Eilers, P.H., A perfect smoother. Analytical chemistry, 2003. 75(14): p. 3631-3636.